

University of Nebraska - Lincoln

DigitalCommons@University of Nebraska - Lincoln

---

Faculty Publications from the Center for Plant  
Science Innovation

Plant Science Innovation, Center for

---

2010

## **$\gamma$ -Zeins are essential for endosperm modification in quality protein maize**

Yongrui Wu  
*Rutgers University*

David R. Holding  
*University of Nebraska, Lincoln, dholding2@unl.edu*

Joachim Messing  
*Rutgers University*

Follow this and additional works at: <https://digitalcommons.unl.edu/plantscifacpub>



Part of the [Plant Sciences Commons](#)

---

Wu, Yongrui; Holding, David R.; and Messing, Joachim, " $\gamma$ -Zeins are essential for endosperm modification in quality protein maize" (2010). *Faculty Publications from the Center for Plant Science Innovation*. 48. <https://digitalcommons.unl.edu/plantscifacpub/48>

This Article is brought to you for free and open access by the Plant Science Innovation, Center for at DigitalCommons@University of Nebraska - Lincoln. It has been accepted for inclusion in Faculty Publications from the Center for Plant Science Innovation by an authorized administrator of DigitalCommons@University of Nebraska - Lincoln.

# $\gamma$ -Zeins are essential for endosperm modification in quality protein maize

Yongrui Wu<sup>a</sup>, David R. Holding<sup>b</sup>, and Joachim Messing<sup>a,1</sup>

<sup>a</sup>Waksman Institute of Microbiology, Rutgers University, Piscataway, NJ 08854; and <sup>b</sup>Department of Agronomy and Horticulture, Center for Plant Science Innovation, University of Nebraska, Lincoln, NE 68588-0665

Edited\* by Ronald L. Phillips, University of Minnesota, St. Paul, MN, and approved May 18, 2010 (received for review April 13, 2010)

**Essential amino acids like lysine and tryptophan are deficient in corn meal because of the abundance of zein storage proteins that lack these amino acids. A natural mutant, *opaque 2* (*o2*) causes reduction of zeins, an increase of nonzein proteins, and as a consequence, a doubling of lysine levels. However, *o2*'s soft inferior kernels precluded its commercial use. Breeders subsequently overcame kernel softness, selecting several quantitative loci (QTLs), called *o2* modifiers, without losing the high-lysine trait. These maize lines are known as "quality protein maize" (QPM). One of the QTLs is linked to the 27-kDa  $\gamma$ -zein locus on chromosome 7S. Moreover, QPM lines have 2- to 3-fold higher levels of the 27-kDa  $\gamma$ -zein, but the physiological significance of this increase is not known. Because the 27- and 16-kDa  $\gamma$ -zein genes are highly conserved in DNA sequence, we introduced a dominant RNAi transgene into a QPM line (CM105*Mo2*) to eliminate expression of them both. Elimination of  $\gamma$ -zeins disrupts endosperm modification by *o2* modifiers, indicating their hypostatic action to  $\gamma$ -zeins. Abnormalities in protein body structure and their interaction with starch granules in the F1 with *Mo2/+; o2/o2;  $\gamma$ RNAi/+* genotype suggests that  $\gamma$ -zeins are essential for restoring protein body density and starch grain interaction in QPM. To eliminate pleiotropic effects caused by *o2*, the 22-kDa  $\alpha$ -zein,  $\gamma$ -zein, and  $\beta$ -zein RNAis were stacked, resulting in protein bodies forming as honeycomb-like structures. We are unique in presenting clear demonstration that  $\gamma$ -zeins play a mechanistic role in QPM, providing a previously unexplored rationale for molecular breeding.**

electron microscopy | stacking of RNAi events | storage organs | opaque phenotype | kernel hardness

**G**rain hardness is a key agronomic trait in maize (*Zea mays* L.) because it provides resistance to damage during harvesting and marketing, as well as to insect and fungal damage. Kernel texture is determined by the relative amounts of hard (vitreous) and soft (opaque) endosperm and there is a positive correlation between zein storage proteins and kernel vitreousness (1). Zeins are a heterogeneous mixture of alcohol-soluble proteins, falling into four classes based on their structure ( $\alpha$ -,  $\beta$ -,  $\gamma$ -, and  $\delta$ -zeins) (2). The zeins extracted with the Osborne method (3) are classified as z1 (19- and 22-kDa  $\alpha$ -zeins) and the cross-linked z2 group (50-, 27-, and 16-kDa  $\gamma$ -zeins, 15-kDa  $\beta$ -zein, and 18- and 10-kDa  $\delta$ -zeins) (4, 5). Zeins are deposited in rough endoplasmic reticulum-delimited protein bodies (PBs) in endosperm cells from around 10 d after pollination (DAP) (6, 7). Alpha- and  $\delta$ -zeins are mainly stored in the center of PBs, and  $\gamma$ - and  $\beta$ -zeins are deposited in the peripheral region (8). The Cys-rich  $\gamma$ - and  $\beta$ -zeins have redundant function in the stabilization of PB morphology (9). The translucency (vitreousness) of the mature kernel is influenced by PB composition and the spatial organization of  $\alpha$ -,  $\beta$ -,  $\gamma$ -, and  $\delta$ -zeins (10–16).

Because zeins are essentially devoid of lysine and tryptophan, their high-level accumulation results in poor grain-protein quality (17, 18). The *opaque2* (*o2*) mutant, identified by Singleton and Jones in the 1920s (19), initially showed great promise in monogastric animal feeding trials because it was shown to have twice the normal levels of lysine and tryptophan (15). The improved nutritional value resulted from much reduced  $\alpha$ -zein accumulation, which paradoxically caused a soft endosperm texture

that ultimately prevented the commercial success of *o2*. Quality protein maize (QPM) was developed by selecting modified *o2* lines with restored vitreous endosperm that maintained the low- $\alpha$ -zein, high-lysine phenotype (20).

Genetic analysis of *o2* modifiers identified several disperse quantitative trait loci (QTLs). Although their molecular identities have remained unknown, QTLs could be correlated with observed increases in 27-kDa  $\gamma$ -zein transcript and protein in QPM (21). Unlike the 22-kDa  $\alpha$ -zein genes, the 27-kDa  $\gamma$ -zein gene is not under the transcriptional control of the *O2* protein (22, 23). Two different QTLs, which are candidates for *o2* modifier genes, affect 27-kDa  $\gamma$ -zein gene expression. The first of these is associated with increased expression (24) and the other is linked to *o15*, a mutation at a different chromosome 7 location (25), which causes decreased 27-kDa  $\gamma$ -zein expression. The first QTL could be a *cis*-acting mutation of the 27-kDa zein gene, and the latter a *trans*-acting factor. In the B73 genome, single-copy  $\gamma$ -zein genes encode the 50-, 27-, and 16-kDa proteins (6). The 27- and 16-kDa  $\gamma$ -zein genes originated from a common progenitor by allotetraploidization and share high DNA and protein-sequence similarity (5). Their proteins amount to about 20 to 25% of total zeins (26); the low abundance 50-kDa  $\gamma$ -zein gene has low similarity to the other two  $\gamma$ -zein genes (6). Although the 16-kDa  $\gamma$ -zein expression is not elevated like the 27-kDa  $\gamma$ -zein gene in QPM, probably because of diverged regulation, their protein products and  $\beta$ -zein have redundant and unique function in protein body stabilization (9). Furthermore, neither the 27-kDa  $\gamma$ -zein-null mutant nor the  $\beta$ -zein RNAi seeds showed any opaque phenotype (9, 27). When the 27- and 16-kDa  $\gamma$ -zeins were knocked-down by  $\gamma$ RNAi, only partial opacity occurred (9). The opacity was strongly intensified when the  $\gamma$ RNAi and  $\beta$ RNAi were combined. The opacity was not caused by reducing the thickness of the vitreous endosperm as in *o2*, but by an incomplete embedding of starch granules in the vitreous area (9). Because the expression of the  $\beta$ -zein gene is also regulated by *O2* (28) and significantly reduced in QPM (29), the amount of  $\gamma$ -zeins would become critical to keep starch granules embedded in the vitreous area. To examine the role of  $\gamma$ -zeins in QPM, we used an RNAi construct designed from the inverted coding sequences of the 27-kDa  $\gamma$ -zein gene to knock down both 27- and 16-kDa  $\gamma$ -zeins by taking advantage of their DNA sequence conservation (9). Indeed, in the progeny with the genotype *Mo2/+; o2/o2;  $\gamma$ RNAi/+* from the cross of QPM with *O2/o2;  $\gamma$ RNAi/+*, the modified phenotype was lost, indicating that the action of the *o2* modifiers is preconditioned by the expression of  $\gamma$ -zeins, which is genetically described as hypostasis. In the resulting endosperm cells, although discrete PBs were still observed, larger, honeycomb-like masses of unseparated PBs were also observed. This indicated that both z1

Author contributions: Y.W. and J.M. designed research; Y.W. performed research; Y.W. and D.R.H. contributed new reagents/analytic tools; Y.W., D.R.H., and J.M. analyzed data; and Y.W., D.R.H., and J.M. wrote the paper.

The authors declare no conflict of interest.

\*This Direct Submission article had a prearranged editor.

<sup>1</sup>To whom correspondence should be addressed. E-mail: [messing@waksman.rutgers.edu](mailto:messing@waksman.rutgers.edu).

This article contains supporting information online at [www.pnas.org/lookup/suppl/doi:10.1073/pnas.1004721107/-DCSupplemental](http://www.pnas.org/lookup/suppl/doi:10.1073/pnas.1004721107/-DCSupplemental).



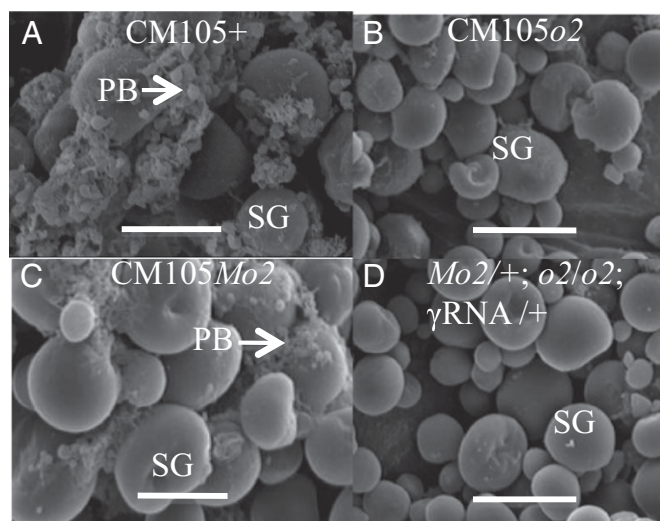


**Fig. 3.** Scanning electron micrographs of protein bodies in different genotypes. (A) CM105+. (B) CM105*o2*. (C) CM105*Mo2*. (D) *Mo2*/+; *o2*/*o2*;  $\gamma$ RNAi/+. (Scale Bars, 10  $\mu$ m.) PB, protein body; SG, starch granules.

A unique effect on PBs was observed when the  $\gamma$ RNAi and the QPM properties were combined in the *Mo2*/+; *o2*/*o2*;  $\gamma$ RNAi/+ genotype. PBs were no longer discrete, but appeared as multi-lobe irregular structures (Fig. 2*E* and Fig. S1*E*). This result has previously been observed in mutants where zeins were not properly processed, like *floury2* (13, 34, 35). Interestingly, when a triple combination of  $\gamma$ RNAi,  $\beta$ RNAi, and QPM was examined, these abnormal PB masses were larger and more frequently observed (Fig. 2*F* and Fig. S1*F*).

#### Scanning Electron Microscopy of Endosperm from $\gamma$ RNAi in QPM.

Further examination of PBs with scanning electron microscopy permits the analysis of the interaction between PBs and starch granules, which is thought to be important in determining kernel vitreousness (36). During endosperm development, starch granules and PBs are embedded in a proteinaceous cytoskeletal matrix (31, 37). In *o2* endosperm, the proteinaceous matrix is almost totally absent, resulting in loose and noncompacted starch granules (Fig. 3*B*), whereas in QPM, a matrix is partially restored (Fig. 3*C*) (31). However, the partial matrix was abolished by knock-down of  $\gamma$ -zeins (Fig. 3*D*). This finding is consistent with its considerable reduction not only in  $\alpha$ -zeins, but also  $\gamma$ - and  $\beta$ -zeins (Fig. 1*C*). In QPM, although PB size, number, and proteinaceous matrix were all reduced compared with wild-type endosperm, these parameters were all considerably larger than in *o2* (Fig. 3*C*) (31). However, when the  $\gamma$ RNAi was introduced into QPM, the resulting genotype *Mo2*/+; *o2*/*o2*;  $\gamma$ RNAi/+ generated the same phenotype as the *o2* mutant (Fig. 3*B* and *D*), where the proteinaceous matrix is completely disrupted, indicating that endosperm modification is abolished.

The elevated accumulation of the 27-kDa  $\gamma$ -zein in QPM endosperm is associated with an increase in the number and size of PBs, and vitreous endosperm formation in the *o2* mutant background. Whether the restoration of the proteinaceous network is related to the elevated expression of 27-kDa  $\gamma$ -zein remains to be seen. Interestingly, uncharacterized opaque mutants, such as *opaque9*, exhibit no reduction in zein accumulation (38), suggesting that they might only have changes in spatial deposition of zeins in PBs, like *floury1* (10), or encode cytoplasm-resident proteins that are necessary for vitreous endosperm formation during kernel maturation. It is possible that such hypothetical proteins are increased in QPM. The modification effects of the

dominantly acting *o2* modifier genes on the soft *o2* phenotype are completely suppressed by the  $\gamma$ RNAi. This shows that  $\gamma$ -zeins are necessary for modification but does not prove that they are alone sufficient. If other genes act in concert with the  $\gamma$ -zeins and increase to allow modification, we propose that actions of these genes are hypostatic to the high expression of  $\gamma$ -zein genes.

**Loss of QPM Kernel Phenotype by Knock-Down of  $\gamma$ -Zeins.** The breeding of QPM lines can easily be monitored by kernel phenotype because modifiers restore the translucency of the kernel that is lost in opaque mutants. In the progeny of CM105*Mo2*  $\times$  (W64*Ao2*  $\times$   $\gamma$ RNAi/+), kernels with the genotype *Mo2*/+; *o2*/*o2*;  $\gamma$ RNAi/+ are not only sharply reduced in  $\alpha$ -zein, but also in  $\gamma$ -zeins. The 27-kDa  $\gamma$ -zein locus is linked to one of the QTLs for endosperm vitreousness (24) and is associated with increased 27-kDa  $\gamma$ -zein expression (21). It is not known if a mutation in the 27-kDa  $\gamma$ -zein gene or promoter is the QTL itself or if its expression is affected by another gene, which is itself the QTL. In either case, the question is raised as to whether the restoration of vitreousness depends on a threshold level of  $\gamma$ -zeins. If enhanced  $\gamma$ -zein levels allows endosperm modification either acting independently or in concert with other *o2* modifiers, its loss should result in reappearance of the soft *o2* phenotype. Indeed, the resulting ear exhibited a 1:3 segregation of opaque and vitreous kernel phenotypes, instead of the 100% vitreous, as would be expected if 27-kDa  $\gamma$ -zein were not necessary for modification (Fig. 4). Progeny kernels carrying the dominant RNAi construct were totally opaque and contained negligible hard endosperm compared with normal and QPM kernels (Fig. 4), although normal kernels with only the  $\gamma$ RNAi showed no or only slight opacity in the crown area (Fig. S2*C*) (9). When the kernels with the genotype *Mo2*/+; *o2*/*o2*;  $\gamma$ RNAi/+ were backcrossed with CM105*Mo2*, progeny exhibited 1:1 segregation of opaque and

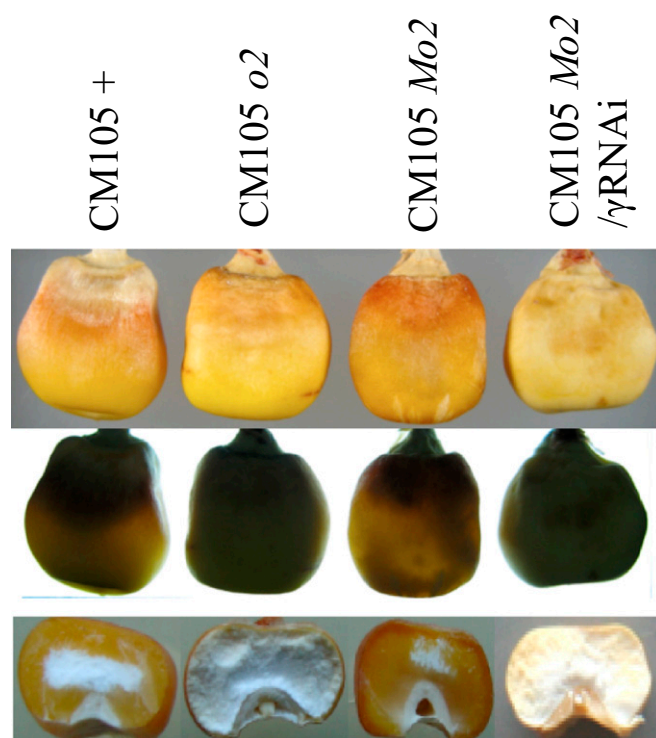


**Fig. 4.** Kernel phenotype for CM105+, CM105*o2*, CM105*Mo2*, and new mutant *Mo2*/+; *o2*/*o2*;  $\gamma$ RNAi/+. Photographs for intact or decapped kernels were taken under incandescent light (Top and Bottom) or with transmitted light (Middle).

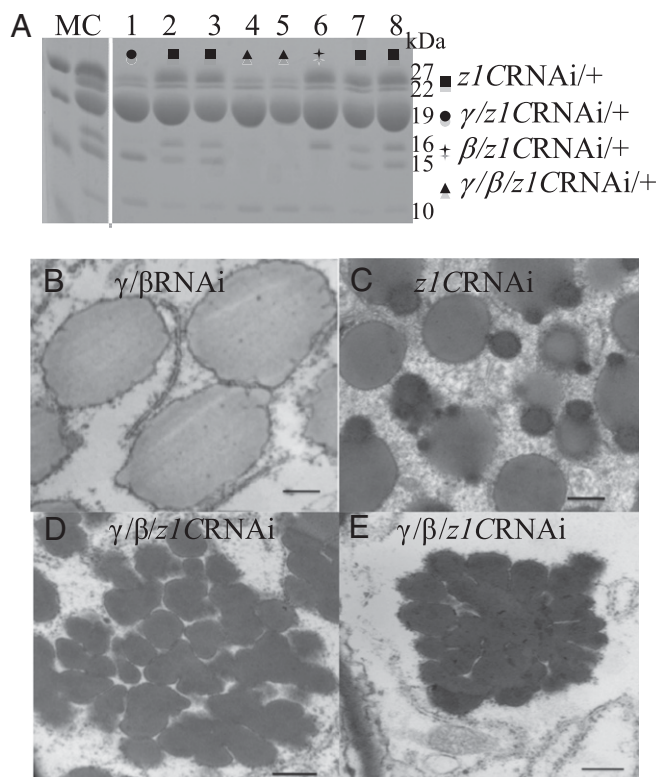


**Fig. 5.** Protein accumulation analysis of the  $\gamma/\beta$  RNAi,  $z1CRNAi$  and their triple-stack ( $z1CRNAi$  used as pollen) and transmission electron micrographs of their protein bodies. (A) Eight kernels dissected from the cross of  $\gamma/\beta$  RNAi  $\times$   $z1CRNAi$  at 18 DAP were analyzed. C, nontransgenic hybrid seed of B and A lines as a control. M, protein markers from top to bottom being 25, 20, 15, and 10 kDa. The slice of protein markers and control run in a different gel was composited with the samples, as indicated by a white line. Total zein loaded in each lane was equal to 500  $\mu$ g of fresh endosperm at 18 DAP. The size for each band is indicated in the "kDa" column. (B–E) Transmission electron micrographs of protein bodies in  $\gamma/\beta$  RNAi stack (B),  $z1CRNAi$  (C), and the stack of  $\gamma/\beta$  RNAi and  $z1CRNAi$  (D and E). (Scale bars, 500 nm.)

vitreous kernel phenotypes (Fig. S3). In such cases, half of the progeny should be homozygous for the 27-kDa  $\gamma$ -zein locus, the major QTL for endosperm modification in QPM. If heterozygosity of this modifiers would be insufficient for a vitreous phenotype, one would expect only a 3:1 segregation because only a quarter of the progeny would be both  $\gamma$ RNAi and homozygous for the modifier. These data confirm the link between the QPM phenotype and  $\gamma$ -zein levels in endosperm. There is a good correlation between transmission electron microscopy observations of PBs and kernel phenotypes.

**Triple Stack of  $z1CRNAi$ ,  $\gamma$ RNAi, and  $\beta$ RNAi Transgenes.** It has been shown that *O2* regulates more genes than just the 22-kDa  $\alpha$ - and  $\beta$ -zeins (39, 40). Furthermore, the QPM phenotype comprises several QTLs, which make quantitative contributions (24). It is therefore conceivable that other factors might be responsible for the disintegration of the subcellular structure of PBs and starch granules in addition to or instead of the regulation of  $\gamma$ - and  $\alpha$ -zein gene expression. To exclude these potential pleiotropic effects, a triple stack of  $z1CRNAi$ ,  $\gamma$ RNAi, and  $\beta$ RNAi transgenes was created (Fig. 5) by reciprocal crosses between a homozygous  $z1CRNAi$  transgenic plant (16) and a plant heterozygous for  $\gamma$ RNAi and  $\beta$ RNAi (9).

Both parental lines were used as references for SDS/PAGE and transmission electron microscopic analysis (Fig. 5A–C and Fig. S4

A and B). At 18 DAP, eight immature kernels were dissected for extraction of total zeins. A nontransgenic Hi II hybrid seed of B  $\times$  A lines was used as a control (Materials and Methods). As expected, all kernels exhibited reduced 22-kDa  $\alpha$ -zein level. Other zeins were not affected, indicating the highly specific action of RNAi (Fig. 5A). Kernels 2, 3, 7, and 8 represented the genotype  $z1CRNAi/+$ , with only the 22-kDa  $\alpha$ -zeins reduced; kernels 4 and 5 represented the genotype  $z1CRNAi/+; \gamma$ RNAi/+;  $\beta$ RNAi/+, with not only the 22-kDa  $\alpha$ -zein but also  $\gamma$ - and  $\beta$ -zeins reduced; kernels 1 and 6 represented the genotype  $z1CRNAi/+; \gamma$ RNAi/+ and  $z1CRNAi/+; \beta$ RNAi/+, respectively, both besides substantially losing the 22-kDa  $\alpha$ -zeins, the  $\gamma$ -zeins or  $\beta$ -zein being knocked down to barely detectable levels as well (Fig. 5A). As expected, the kernels with the triple stack of the  $z1CRNAi$ ,  $\gamma$ RNAi, and  $\beta$ RNAi showed a full opaque phenotype, similar to kernels with  $z1CRNAi$  alone (Fig. S2E) (9, 16, 41), indicating that a significant loss of  $\alpha$ -zeins is sufficient to cause kernel opacity alone (Fig. S2E).

Most PBs in the triple stack of  $z1CRNAi$ ,  $\gamma$ RNAi, and  $\beta$ RNAi had an irregular shape similar to the double stack of  $\beta$ RNAi and  $\gamma$ RNAi (Fig. 5B, D, and E and Fig. S4A–C) (9). Moreover, the mature PBs were no longer discrete but consisted of masses that appeared to comprise tens of unseparated PBs, with diameters considerably larger than the normal 1- to 2- $\mu$ m size (Fig. 5D and E and Fig. S4C). This finding was similar to the observations in the stack of QPM and  $\gamma$ RNAi (Fig. 2E and F and Fig. S1E and F), only more severe. Scanning electron microscopy revealed that these PB masses could still interact with starch grains (Fig. S5). Because of the abnormal size and shape of PB masses and their unknown surface characteristics, it seems that interactions with starch grains are not able to contribute to the formation of a vitreous endosperm upon desiccation (Fig. 6).

**Mechanism of PB Aggregation.** Undoubtedly, one effect of the  $\gamma$ RNAi effect on QPM is to prevent accretion of zeins into normally shaped endoplasmic reticulum-derived PBs. Other mutants with similar clumped PBs always show the opaque endosperm phenotype (9, 11, 12, 14). What could cause this abnormal PB phenotype? Our use of an RNAi transgene permits us to exclude the pleiotropic effects of the conventional *trans*-acting factors, like *O2*. Lobing and failed separation of PBs occurs when both Cys-rich ( $\gamma$ - and  $\beta$ -) and Cys-poor (22-kDa  $\alpha$ -) zeins were reduced simultaneously, suggesting that the phenotype is associated with a quantitative and qualitative loss of zeins, rather than a reduction only in either the 22-kDa  $\alpha$ -zein or  $\gamma$ - and  $\beta$ -zeins (Fig. 5B and C and Fig. S4A and B). Protein levels alone cannot be the basis for the phenotype because, although both triple-stacked RNAi and *o2* have dramatically reduced total zeins, *o2* has discrete PBs. The difference is that the  $\gamma$ -zeins reach normal levels in the *o2* mutant but are lost in the triple stack. Therefore, lobed and unseparated PB masses occur when both  $\alpha$ - and  $\gamma$ -/ $\beta$ -zein classes are reduced to low levels. It is possible that the residual 19-kDa  $\alpha$ -zeins in the QPM  $\times$   $\gamma$ RNAi and the  $\alpha$ -,  $\beta$ -, and  $\gamma$ -RNAi triple stack prevent PB separation because of the loss of encapsulating  $\gamma$ -zeins, and that their difference in relative severity relates to the amount of residual  $\alpha$ -zeins. In comparison, *o2* has normal discrete PBs because residual  $\alpha$ -zeins are encapsulated in  $\gamma$ -zeins. This explanation for disrupted PB separation is summarized in Table 1.

Interestingly, the morphology and organization of PBs in this triple stack is reminiscent of *fl2*, where protein-body separation is also disrupted (34); *fl2* is linked to a single 22-kDa zein gene with an amino acid change that prevents processing of the signal peptide, thereby slowing down the deposition of other zeins into PBs. During early PB formation, only  $\gamma$ - and  $\beta$ -zeins are deposited (8), and this explains the variable penetrance of the phenotype in relation to the PB size gradient between the subaleurone layer and the central portion of the endosperm (34). The fused PBs observed in our triple RNAi stack may arise by the same mechanism as in *fl2*, as both have reduced accumulation of  $\alpha$ -zeins, as

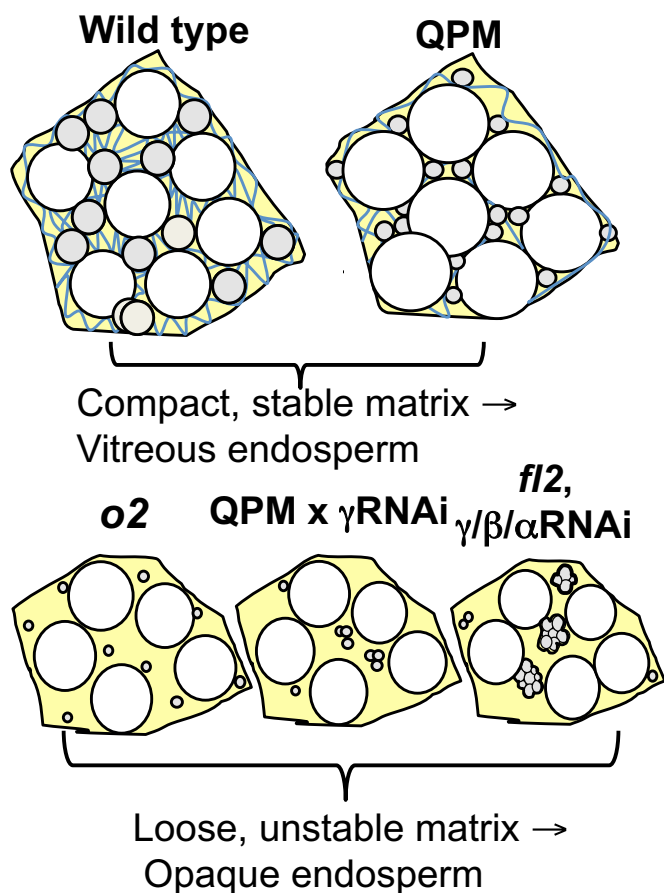


**Fig. 6.** Model for vitreous endosperm formation in which midmaturation stage (18 DAP) starchy endosperm cells are depicted. PBs are represented with gray spheres, starch grains with white spheres, and proteinaceous matrix with blue lines. In wild-type and QPM, compact stable matrices give rise to glass-like, vitreous endosperm at maturity. In opaque mutants and dominant RNAi low-zein lines, small, sparse, or lobed unseparated PBs produce loose, unstable matrices, which shatter during desiccation, producing an opaque texture at maturity.

well as  $\gamma$ - and  $\beta$ -zeins. A common feature of *fl2* and the triple stack may be their “out of context” accumulation of  $\alpha$ -zeins, where the semidominant mutant *fl2*  $\alpha$ -zein or large amounts of the 19-kDa  $\alpha$ -zeins lack the encapsulating 22-kDa  $\alpha$ - and  $\gamma$ -zeins. An unknown mutation causes similarly aggregated PBs in a highly digestible sorghum cultivar (42, 43), inviting speculation that it is caused by a semidominant kafirin mutation analogous to *floury 2*.

It has also been shown that PBs in endosperm cells are not randomly distributed but are evenly distributed around starch granules embedded in a protein matrix rich in EF-1 $\alpha$  and cytoskeletal elements, such as actin and microtubules (37). Indeed, seed architecture could have evolved to use the cytoskeletal network in the distribution of PBs. If this is the case, the interaction between PBs and the cytoskeleton could depend on an appropriate internal PB structure, which depends on the timely accumu-

lation of the correct proportions of  $\gamma$ -,  $\beta$ -, and  $\alpha$ -zeins. In *o2* endosperm, this balance is upset both in terms of PB size, shape, and the surrounding protein matrix (Fig. 6). These parameters are only partially restored to wild-type in QPM but result in kernels that are as vitreous as wild-type. In this case, it is possible that the increased 27 kDa  $\gamma$ -zein allows the accumulation of small but numerous PBs that, along with the proteinaceous matrix, participate in a mature endosperm structure whose vitreousness perhaps develops in a somewhat distinct manner from wild-type (Fig. 6). Whether similar or distinct to wild-type endosperm maturation, we are unique in showing that an increase in  $\gamma$ -zein is essential for endosperm modification in QPM.

## Materials and Methods

**Genetic Stocks.** Maize inbred line CM105+, its *o2* mutant CM105o2, and the modified *o2* mutant CM105Mo2 have been reported previously (24). CM105 wild-type, *o2* and *Mo2* were grown in the field in Lincoln, Nebraska in summer, 2009. The *z1CRNAi* (for knockdown of the 22-kDa  $\alpha$ -zeins),  $\gamma$ RNAi (for knockdown of the 27- and 16-kDa  $\gamma$ -zeins), and  $\beta$ RNAi (for knockdown of the 15-kDa  $\beta$ -zein) were generated previously (9, 16).

**Total Zein Extraction.** Immature kernels at 18 DAP were harvested. The embryos were saved for extraction of DNA individually. The genotype of each kernel with respect to the  $\gamma$ RNAi gene was confirmed by PCR with primer pair 5'-ACAACCACTACTCTGAGCAC-3' and 5'-ATTAAGCTTTGCAGG-TCACTGGATTGG-3', which has been described elsewhere (9). Each endosperm was cut into two halves. One was fixed for transmission or scanning electron microscopy. The other half ( $\approx 50$  mg) was used for zein extraction. The finely ground endosperm was mixed and vortexed with 400  $\mu$ L of 70% ethanol/2% 2-mercaptoethanol (vol/vol), then kept on the bench at room temperature for 2 h; the mixture was centrifuged at 13,000 rpm (Eppendorf, Centrifuge 5417C) in a microfuge for 10 min, then 200  $\mu$ L of the supernatant liquid was transferred to a new tube; 10  $\mu$ L of 10% SDS was added to the extract, the mixture was dried by vacuum, and resuspended in 100  $\mu$ L of distilled water. Next, 2  $\mu$ L (equal to 500- $\mu$ g endosperm powder) of each sample was analyzed by 15% SDS/PAGE gel.

**Stacking of Zein RNAi Transgenes.** The QPM CM105Mo2 was pollinated by the F1 progeny of W64Ao2  $\times$   $\gamma$ RNAi or W64Ao2  $\times$  ( $\gamma$ RNAi  $\times$   $\beta$ RNAi).

The triple stack of the *z1CRNAi*,  $\gamma$ RNAi, and  $\beta$ RNAi was generated from reciprocal crosses between a homozygous *z1CRNAi* plant and a double stack of  $\gamma$ RNAi and  $\beta$ RNAi.

**Transmission and Scanning Electron Microscopy.** Previously published methods were used with some modifications (34, 44). Two 2-mm thick sections were sliced perpendicular to the aleurone layer to include the pericarp, aleurone, and 10 to 20 cell layers of the endosperm. All these slices were fixed in 5% glutaraldehyde in 0.1 M sodium cacodylate buffer, PH 7.4, containing 2% sucrose, in a 2-mL tube. Fixation was kept at 4  $^{\circ}$ C overnight and for another 3 h at room temperature. The tissues were rinsed for 2 to 3 h with several changes of 0.1 M sodium cacodylate buffer containing decreasing amounts of sucrose. They were then postfixed in buffered 1% osmium tetroxide at 4  $^{\circ}$ C overnight followed by dehydration in a graded series of acetone washings and embedded in epon resin.

For electron microscopy, 90-nm thin sections were cut on a Leica EM UC 6- $\mu$ L tramicrotome. Sectioned grids were stained with saturated solution of uranyl acetate and lead citrate. Sections were analyzed at 80 Kv with a Philips CM 12 transmission electron microscope.

For scanning electron microscopy, the dehydrated 18-DAP samples were dried to a critical point, using CO<sub>2</sub> in a dryer (Balzers CPD 020); the dried samples were mounted on the surface of a brass disk using double-sided adhesive silver-tape, coated with gold/palladium by a sputter coating unit (Balzers CSD 004) and viewed on a scanning electron microscope (Amray 1830 I).

**Table 1.** Effect of zein disruptions on protein-body morphology

Genotype	Zeins present	Zein interactions	Phenotype
<i>o2</i>	Low levels of 19- and 22- $\alpha$ ; normal $\gamma$	Residual $\alpha$ are encased in $\gamma$	No PB lobing
QPM $\gamma$ RNAi	Low levels of 19- and 22- $\alpha$ ; low $\gamma$	Residual $\alpha$ are not encased in $\gamma$	Moderate PB lobing
Triple stack (22- $\alpha$ , $\gamma$ , and $\beta$ RNAi)	Moderate 19- and low 22- $\alpha$ ; low $\gamma$	Lots of 19 $\alpha$ are not encased in $\gamma$	More severe PB lobing

**ACKNOWLEDGMENTS.** We thank Brian Larkins and his past laboratory members for generating the CM105 Mo2 material. The research described

in this article was supported by the Selman A. Waksman Chair in Molecular Genetics.

1. Moose SP, Dudley JW, Rocheford TR (2004) Maize selection passes the century mark: A unique resource for 21st century genomics. *Trends Plant Sci* 9:358–364.
2. Esen A (1987) A proposed nomenclature for the alcohol-soluble proteins (zeins) of maize (*Zea mays* L.). *J Cereal Sci* 5:117–128.
3. Osborne TB (1891) Process of extracting zein. US Patent 456773.
4. Sodek L, Wilson CM (1971) Amino acid composition of proteins isolated from normal, opaque-2, and floury-2 corn endosperms by a modified Osborne procedure. *J Agric Food Chem* 19:1144–1150.
5. Xu JH, Messing J (2008) Organization of the prolamin gene family provides insight into the evolution of the maize genome and gene duplications in grass species. *Proc Natl Acad Sci USA* 105:14330–14335.
6. Woo YM, Hu DW, Larkins BA, Jung R (2001) Genomics analysis of genes expressed in maize endosperm identifies novel seed proteins and clarifies patterns of zein gene expression. *Plant Cell* 13:2297–2317.
7. Larkins BA, Hurkman WJ (1978) Synthesis and deposition of zein in protein bodies of maize endosperm. *Plant Physiol* 62:256–263.
8. Lending CR, Larkins BA (1989) Changes in the zein composition of protein bodies during maize endosperm development. *Plant Cell* 1:1011–1023.
9. Wu Y, Messing J (2010) RNA interference-mediated change in protein body morphology and seed opacity through loss of different zein proteins. *Plant Physiol* 153:337–347.
10. Holding DR, et al. (2007) The maize *floury1* gene encodes a novel endoplasmic reticulum protein involved in zein protein body formation. *Plant Cell* 19:2569–2582.
11. Kim CS, et al. (2004) A defective signal peptide in a 19-kD alpha-zein protein causes the unfolded protein response and an opaque endosperm phenotype in the maize De\*-B30 mutant. *Plant Physiol* 134:380–387.
12. Coleman CE, et al. (1997) Expression of a mutant alpha-zein creates the *floury2* phenotype in transgenic maize. *Proc Natl Acad Sci USA* 94:7094–7097.
13. Coleman CE, Lopes MA, Gillikin JW, Boston RS, Larkins BA (1995) A defective signal peptide in the maize high-lysine mutant *floury 2*. *Proc Natl Acad Sci USA* 92:6828–6831.
14. Kim CS, et al. (2006) The maize Mucronate mutation is a deletion in the 16-kDa gamma-zein gene that induces the unfolded protein response. *Plant J* 48:440–451.
15. Mertz ET, Bates LS, Nelson OE (1964) Mutant gene that changes protein composition and increases lysine content of maize endosperm. *Science* 145:279–280.
16. Segal G, Song R, Messing J (2003) A new opaque variant of maize by a single dominant RNA-interference-inducing transgene. *Genetics* 165:387–397.
17. Osborne TB, Mendel LB (1914) Nutritional properties of proteins of the maize kernel. *J Biol Chem* 18(1):1–16.
18. Osborne TB, Mendel LB (1914) Amino-acids in nutrition and growth. *J Biol Chem* 17:325–349.
19. Emerson RA, Beadle GE, Fraser AC (1935) A summary of linkage studies in maize. *Cornell University Agricultural Experiment Station Memoir* 180:1–83.
20. Vasal SK, Villegas E, Bjarnason M, Gelaw B, Goertz P (1980) Genetic modifiers and breeding strategies in developing hard endosperm opaque 2 materials. *Improvement of Quality Traits of Maize for Grain and Silage Use*, eds Prollmer MG, Phillips RH (Martinus Nijhoff, London), pp 37–73.
21. Geetha KB, Lending CR, Lopes MA, Wallace JC, Larkins BA (1991) Opaque-2 modifiers increase gamma-zein synthesis and alter its spatial distribution in maize endosperm. *Plant Cell* 3:1207–1219.
22. Schmidt RJ, Ketudat M, Aukerman MJ, Hoschek G (1992) Opaque-2 is a transcriptional activator that recognizes a specific target site in 22-kD zein genes. *Plant Cell* 4:689–700.
23. Ueda T, et al. (1992) Mutations of the 22- and 27-kD zein promoters affect trans-activation by the Opaque-2 protein. *Plant Cell* 4:701–709.
24. Holding DR, et al. (2008) Genetic analysis of opaque2 modifier loci in quality protein maize. *Theor Appl Genet* 117:157–170.
25. Dannenhoffer JM, Bostwick DE, Or E, Larkins BA (1995) Opaque-15, a maize mutation with properties of a defective opaque-2 modifier. *Proc Natl Acad Sci USA* 92:1931–1935.
26. Thompson GA, Larkins BA (1994) Characterization of zein genes and their regulation in maize endosperm. *The Maize Handbook*, eds Freeling M, Walbot V (Springer-Verlag, New York), pp 639–647.
27. Holding DR, Larkins BA (2009) Zein storage proteins. *Molecular Genetic Approaches to Maize Improvement*, eds Kriz AL, Larkins BA (Springer, Berlin), pp 269–286.
28. Cord Neto G, et al. (1995) The involvement of Opaque 2 on beta-prolamin gene regulation in maize and Coix suggests a more general role for this transcriptional activator. *Plant Mol Biol* 27:1015–1029.
29. Or E, Boyer SK, Larkins BA (1993) Opaque2 modifiers act post-transcriptionally and in a polar manner on gamma-zein gene expression in maize endosperm. *Plant Cell* 5:1599–1609.
30. Wu Y, Goettel W, Messing J (2009) Non-Mendelian regulation and allelic variation of methionine-rich delta-zein genes in maize. *Theor Appl Genet* 119:721–731.
31. Gibbon BC, Wang X, Larkins BA (2003) Altered starch structure is associated with endosperm modification in Quality Protein Maize. *Proc Natl Acad Sci USA* 100:15329–15334.
32. Wang X, Woo YM, Kim CS, Larkins BA (2001) Quantitative trait locus mapping of loci influencing elongation factor 1alpha content in maize endosperm. *Plant Physiol* 125:1271–1282.
33. Wolf MJ, Khoo U, Seckinger HL (1967) Subcellular structure of endosperm protein in high-lysine and normal corn. *Science* 157:556–557.
34. Lending CR, Larkins BA (1992) Effect of the *floury-2* locus on protein body formation during maize endosperm development. *Protoplasma* 171:123–133.
35. Zhang F, Boston RS (1992) Increases in binding protein (BiP) accompany changes in protein body morphology in three high-lysine mutants of maize. *Protoplasma* 171:142–152.
36. Duvick DN (1961) Protein granules of maize endosperm cells. *Cereal Chem* 38:374–385.
37. Clore AM, Dannenhoffer JM, Larkins BA (1996) EF-1[alpha] is associated with a cytoskeletal network surrounding protein bodies in maize endosperm cells. *Plant Cell* 8:2003–2014.
38. Balconi C, Berardo C, Reali A, Motto M (1998) Variation in protein fractions and nitrogen metabolism of developing normal and opaque endosperm mutants of maize. *Maydica* 43:195–203.
39. Hunter BG, et al. (2002) Maize opaque endosperm mutations create extensive changes in patterns of gene expression. *Plant Cell* 14:2591–2612.
40. Bass HW, Webster C, O'Brien GR, Roberts JK, Boston RS (1992) A maize ribosome-inactivating protein is controlled by the transcriptional activator Opaque-2. *Plant Cell* 4:225–234.
41. Huang S, et al. (2004) Improving nutritional quality of maize proteins by expressing sense and antisense zein genes. *J Agric Food Chem* 52:1958–1964.
42. Oria MP, Hamaker BR, Axtell JD, Huang CP (2000) A highly digestible sorghum mutant cultivar exhibits a unique folded structure of endosperm protein bodies. *Proc Natl Acad Sci USA* 97:5065–5070.
43. Tesso T, Hamaker BR, Ejeta G (2008) Sorghum protein digestibility is affected by dosage of mutant alleles in endosperm cells. *Plant Breeding* 127:579–586.
44. Burr B, Burr FA (1976) Zein synthesis in maize endosperm by polyribosomes attached to protein bodies. *Proc Natl Acad Sci USA* 73:515–519.

# Supporting Information

Wu et al. 10.1073/pnas.1004721107

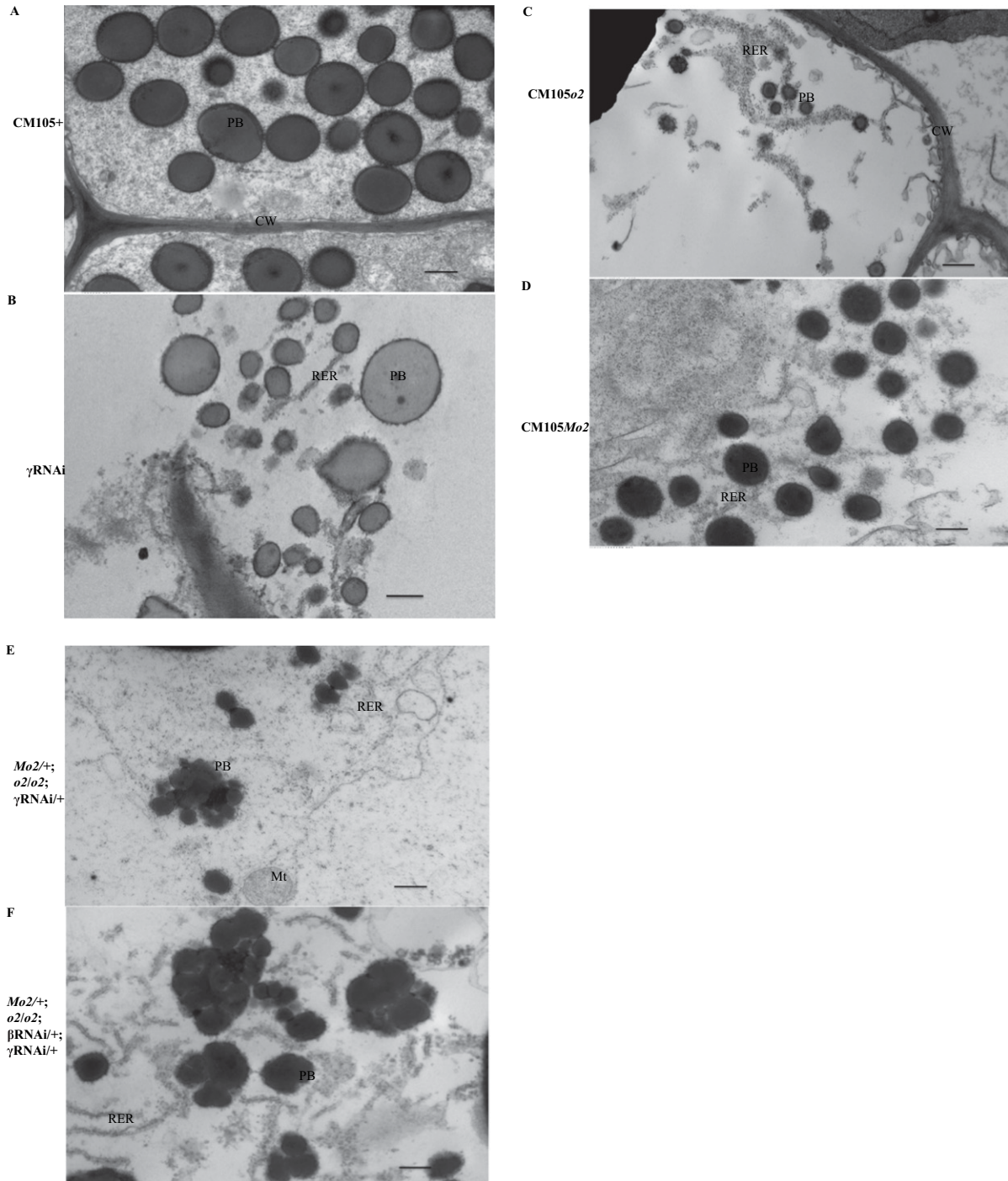


**Fig. S1.** Transmission electron micrographs of protein bodies in different genotypes with wider field view at 18 d after pollination. (A) CM105+. (B)  $\gamma$ RNAi. (C) CM105o2. (D) CM105Mo2. (E)  $Mo2/+; o2/o2; \gamma$ RNAi/+. (F)  $Mo2/+; o2/o2; \beta$ RNAi/+;  $\gamma$ RNAi/+. (Scale bars, 500 nm.) CW, cell wall; Mt, mitochondria; PB, protein body; RER, rough endoplasmic reticulum.



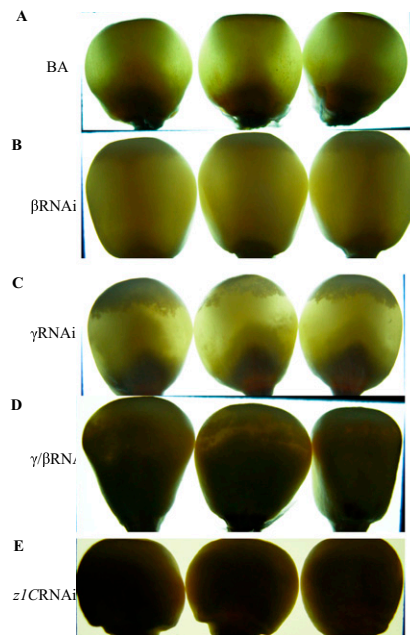


**Fig. S2.** Kernel opacity of the RNAi mutants. (A) Nontransgenic hybrid of B  $\times$  A lines. (B)  $\beta$ RNAi. (C)  $\gamma$ RNAi. (D)  $\beta/\gamma$ RNAi. (E) *z1*CRNAi.

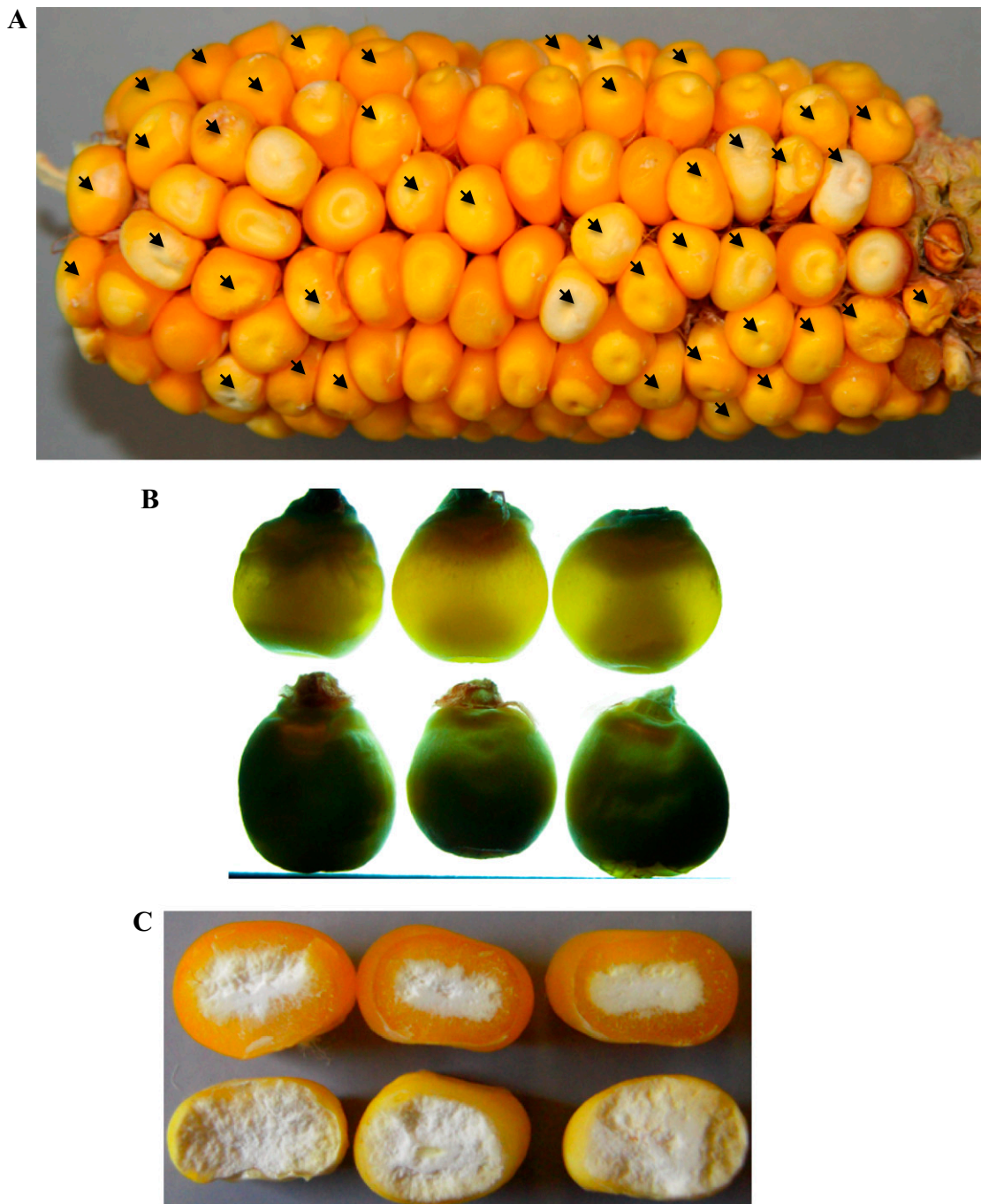


**Fig. 53.** Ear and kernel phenotype resulting from *CM105Mo2* × *Mo2/+*; *o2/o2*;  $\gamma$ RNAi+. (A) Ear phenotype showing 1:1 ratio of vitreous and opaque kernels; opaque kernels are indicated by arrows. (B) Three representative vitreous and opaque kernels from the ear photographed on the light box. (C) Three representative vitreous and opaque kernels from the ear were truncated and photographed under the natural light.

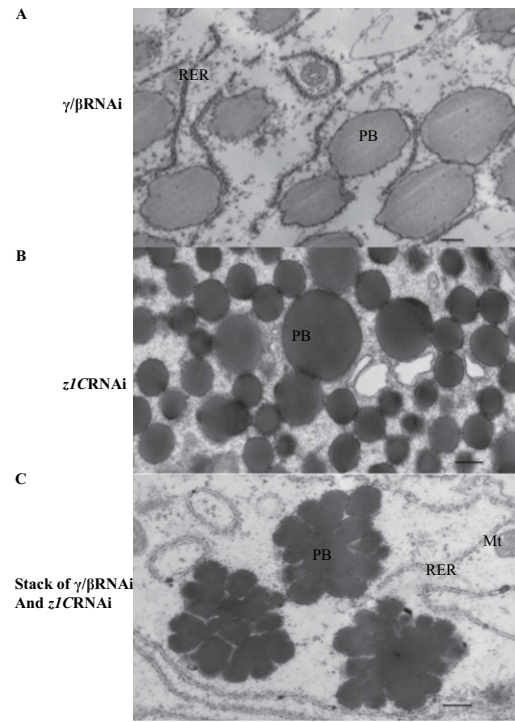


**Fig. S4.** Transmission electron micrographs of protein bodies in different RNAi mutants with wider field view at 18 d after pollination. (A)  $\gamma/\beta$ RNAi. (B)  $z\zeta$ CRNAi. (C) Stack of  $\gamma/\beta$  RNAi and  $z\zeta$ CRNAi. (Scale bars, 500 nm.) Mt, mitochondria; PB, protein body; RER, rough endoplasmic reticulum.

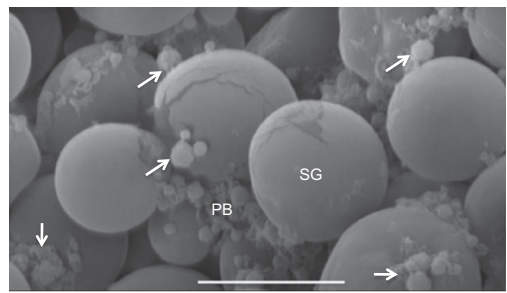


**Fig. S5.** Scanning electron micrographs of the protein bodies from the triple stack of the  $z\zeta$ CRNAi and  $\gamma/\beta$ RNAi (the  $z\zeta$ CRNAi used as pollen) at 18 d after pollination. (Scale bar, 10  $\mu\text{m}$ .) SG, starch granules; PB, protein body. Unseparated PBs are indicated by arrows.